EFDA–JET–PR(07)09

A. Casati, P. Mantica, D. Van Eester, N. Hawkes, F. Imbeaux, E. Joffrin,
A. Marinoni, F. Ryter, A. Salmi, T. Tala, P. De Vries
and the JET EFDA contributors

Critical Temperature Gradient Length Signatures in Heat Wave Propagation Across Internal Transport Barriers in JET

Critical Temperature Gradient Length Signatures in Heat Wave Propagation Across Internal Transport Barriers in JET

A. Casati[1], P. Mantica[2], D. Van Eester[3], N. Hawkes[4], F. Imbeaux[5], E. Joffrin[5], A. Marinoni[6], F. Ryter[7], A. Salmi[8], T. Tala[9], P. De Vries[4]
and the JET EFDA contributors*

[1]*Dipartimento di Ingegneria Nucleare, Politecnico di Milano, Via Ponzio 34/3, 20133 Milano Italy*
[2]*Istituto di Fisica del Plasma 'P. Caldirola', Associazione Euratom-ENEA-CNR, Via Cozzi 53, 20125 Milano, Italy*
[3]*LPP-ERM/KMS, Association Euratom-Belgian State, TEC, B-1000 Brussels, Belgium*
[4]*Culham Science Centre, EURATOM/UKAEA Fusion Association, Abingdon OX14 3DB, UK*
[5]*Association Euratom-CEA, CEA-DSM-DRFC Cadarache, 13108, St Paul-lez-Durance Cedex, France*
[6]*Association Euratom-ConfÈdÈration Suisse, CRPP, EPFL, CH 1015, Lausanne, Switzerland*
[7]*Max-Planck Insitut fur Plasmaphysik, Euratom Association, 85748 Garching, Germany*
[8]*Helsinki Univ. of Technology, Association Euratom-TEKES, P.O. Box 2200, Finland*
[9]*Association Euratom-TEKES, VTT, P.O. Box 1000, FIN-02044 VTT, Finland*
** See annex of M.L. Watkins et al, "Overview of JET Results ", (Proc. 21st IAEA Fusion Energy Conference, Chengdu, China (2006)).*

Preprint of Paper to be submitted for publication in
Physics of Plasmas

ABSTRACT

New results on electron heat wave propagation using ICRH power modulation in JET plasmas characterized by Internal Transport Barriers (ITB) are presented. The heat wave generated outside the ITB and travelling across it, always experiences a strong damping in the ITB layer, demonstrating a low level of transport and loss of stiffness. In some cases, however, the heat wave is strongly inflated in the region just outside the ITB, showing features of convective-like behaviour. In other cases, a second maximum in the perturbation amplitude is generated close to the ITB foot. Such peculiar types of behaviour can be explained on the basis of the existence of a critical temperature gradient length for the onset of turbulent transport. Convective-like features appear close to the threshold (i.e. just outside the ITB foot) when the value of the threshold is sufficiently high, with a good match with theoretical predictions of Trapped Electron Mode thresholds. The appearance of a second maximum is due to the oscillation of the temperature profile across the threshold in the case of a weak ITB. Simulations with an empirical critical gradient length model and with the theory based GLF23 model are presented. The difference with respect to previous results of cold pulse propagation across JET ITBs is also discussed.

1. INTRODUCTION

The use of Internal Transport Barriers (ITBs) to achieve improved core energy confinement in tokamaks is presently under investigation as a possible alternative scenario for ELMy H-mode, with the prospective of steady-state operation [1]. An ITB is generally defined as an internal region of the plasma where turbulent transport is drastically reduced, leading to a local steepening of the temperature as well as of the pressure profiles, with associated generation of bootstrap current.
Although large progress has been made in understanding and controlling ITBs [2-4], several questions concerning ITBs still lack a definitive or convincing answer today. Perturbative studies of ITBs, providing dynamic information on the changes of propagation of a heat wave inside and near an ITB layer, could provide more insight into ITB physics. Such results are not as common as in conventional L- or H-mode scenarios, as they require strong long-lasting ITBs and suitable perturbative techniques, such as the modulation of locally deposited power. In JET such studies are feasible due to the possibility of forming strong ITBs by q profile reversal by Lower Hybrid current drive and sustaining them by NBI heating. ICRH (when choosing conditions favouring Mode Conversion heating) can provide modulated source of localized electron power to probe the ITBs [5, 6]. A recent overview about the physics and the most relevant results of perturbative transport studies can be found in Ref.7.

One important factor behind the success of perturbative techniques in understanding transport in conventional scenarios is the use of the theoretical prediction of the existence of a threshold in the inverse critical gradient length $R/L_T=R|\nabla T|/T$ for the onset of turbulent transport as the key ingredient for the interpretation of the experimental results. Direct evidence of the existence of a threshold has been obtained in ASDEX-Upgrade [8, 9] and a set of data consistent with this concept has been

collected on several machines [10-13]. In this paper, it will be shown that the concept of critical gradient length plays a key role also in explaining the apparently odd results obtained in JET for heat wave propagation in ITB plasmas, thereby, providing further evidence that a critical gradient mechanism is indeed at play.

In section II, a short description of the experimental set-up is provided. In section III, the power modulation results in ITB plasmas showing purely diffusive propagation of the heat waves are presented and successfully simulated using the first principle GLF23 model. Sections IV and V show unexpected evidence, observed for the first time in JET, apparently strongly deviating from the usual diffusive behaviour through a clear amplification of the heat wave whilst propagating away from the source or the formation of a double maximum of the perturbation amplitude. Both the "standard" results of section III and the "anomalous" results of sections IV and V have been successfully modelled using a semi-empirical critical gradient length model, depending on the value of the threshold inside and outside the ITB layer. Comparison with theoretical predictions for electrostatic TEM modes threshold based on linear gyro-kinetic simulations is also discussed. Section VI discusses the comparison between these results from power modulation and previous, apparently different, results for cold pulse propagation in ITBs [14]. Again, the concept of critical gradient length allows the reconciliation of both perturbative results within the same interpretative framework. Finally, section VII summarizes the conclusions.

2. EXPERIMENTAL SET-UP

JET plasmas with toroidal field $B_T \sim 3.25\text{-}3.6$ T, plasma current $I_p \sim 2\text{-}2.5$ MA ($q_{95} \sim 7$), elongation $k_a \sim 1.73$, triangularity (averaged lower and upper) $\delta \sim 0.21$ and density $n_{e0} \sim 2.5\text{-}3.5\times10^{19}$ m^{-3} have been used as targets. LH power ~ 2-3MW was applied in the preheat phase (t=2-4s). Then, from t=4s to t=10s, up to 18MW of NBI power and 5MW of ICRH power modulated with half depth at 20 Hz with duty cycle 60% were applied. Typical heating scheme and evolution of the main plasma parameters are reported for JET62077 in Fig.1. Henceforth plasma discharges will be labelled by 'tokamak-shot number'.

The scheme of Mode Conversion (MC) has been adopted [15], in D plasmas with ^{3}He concentration ~20%, in order to provide a direct and localized electron power source at the ion-ion hybrid layer. At concentration of ~20% and for the parameters typical for the here discussed experiments, about 80% of the modulated power is absorbed by the electrons, half via MC and half in the centre via Fast Wave Landau Damping (FWLD). The former typically has a narrow deposition profile while that of the latter is relatively broad. Collisional coupling with ions, giving an additional modulated electron term, has been estimated by simulations to be completely negligible because of the small perturbation amplitudes on both T_e and T_i ($<\sim \pm 100$eV). T_e has been measured by the 96 channels Electron Cyclotron Emission (ECE) heterodyne radiometer installed at JET, characterized by a radial resolution of about 2 cm and by an acquisition frequency up to 3kHz. The q profile is measured by Motional Stark Effect (MSE), ion temperature profiles by Charge Exchange and n_e

profiles by LIDAR Thomson scattering and interferometry. Standard Fast Fourier Transform (FFT) expansion of T_e signals yields profiles of amplitude A and phase φ of the electron heat wave at various harmonics. The FFT time interval is often limited to few modulation cycles, because of the presence of rather frequent MHD crashes that characterize ITB plasmas; this effect could be the origin of spurious peaks located close to the barrier, leading to an erratic interpretation of the perturbative analysis [6]. Hence, time intervals must be chosen to carefully avoid the MHD crashes.

3. DIFFUSIVE HEAT WAVE PROPAGATION IN JET ITB PLASMAS

The first remarkable results of perturbative transport in JET ITB plasmas have been reported in Ref. 5. These experiments have clearly shown dramatic changes in the propagation of electron heat waves when meeting the barrier, which behaves like a well localized narrow layer characterized by sub-critical transport with respect to turbulence onset and loss of stiffness. A typical result from Ref. 5 is shown in Fig.2 both in presence (Fig.2b) and absence (Fig.2c) of the transport barrier. Errors bars on A and φ have been calculated including random noise at the experimental level on simulated T_e time traces and evaluating mean and standard deviation. The presence of small MHD disturbances makes that core channels are plagued by a higher noise level than channels well outside the inversion radius. Analogous error bars for the following similar discharges will be omitted for reasons of clearness. The adopted power deposition scheme leads to the presence of two heat waves: the first one associated with FWLD propagating from the centre of the plasma to the ITB, while the second one, due to MC, travelling from the outside towards the barrier. The smooth nature of heat waves propagation induced by the power modulation (visible in absence of ITB Fig.2c) is radically changed by the presence of a transport barrier. In this case (Fig.2b) the modulation amplitude profile reveals a very strong damping of both electron heat waves meeting the ITB; on the other side also the slope of phase coefficients shows a sharp rise, particularly evident at the top of the high ∇T_e region. Experiments like the one in Fig.2 allow us to conclude that internal transport barriers are localized layers with very low χ_e, embedded in a higher χ_e plasma. Even more significantly, the fact that the perturbations' propagation is regulated by the incremental diffusivity $\chi_e^{hp} = -\partial q_e / n_e \partial \nabla T_e$ instead of the ordinary power balance value $\chi_e^{pb} = -q_e / n_e \nabla T_e$, allows to conclude that the barrier is a region also of very low χ_e^{hp} and therefore has become fully sub-critical with respect to the turbulence threshold, which is higher than in conventional plasmas, with a consequent complete loss of stiffness. In the cases reported in Ref. 5, the observed dynamics of electron heat perturbations is fully consistent with the expected diffusive behaviour of transport, as also verified in similar experiments for standard L and H mode plasmas [16-18]. Diffusive propagation implies that the modulation amplitude can only decrease away from the position where power is effectively deposited, which is precisely marked by the minimum of φ of the FFT expansion. Therefore with diffusive transport the maximum of A and the minimum of φ coincide, as indeed observed in Fig.2 both with and without ITB. Here and in the following we focus on the first harmonics of the FFT expansion, which is always well above the noise level.

Till today several attempts to model ITB modulation results with several transport models have been carried out [17,19,6]. So far none of these models yielded fully satisfactory results. One of the semi-empirical transport models more successfully applied is the Critical Gradient Model (CGM)[20,11]; this introduces a turbulent heat diffusivity with respect to a residual transport, which sets in above an arbitrary turbulence threshold and is regulated by a stiffness level. This crude model has been proved to be capable of reproducing the damping of the heat waves by ITBs observed in perturbative experiments: this is due to the assumption of a threshold profile whose values are considerably increased inside the ITB region with respect to the rest of plasma [5], implying a sub-critical transport and very low χ_e^{hp} inside the barrier. This is obviously a huge oversimplification that leaves completely out of consideration the turbulence stabilisation mechanisms responsible for the increase of threshold inside the ITB. Therefore further attempts have been made to simulate the results using the theory based GLF23 model [21-24]. Here we present results of simulations that for the first time qualitatively reproduce the experimental results of Fig.2.

Predictive (solving equations for T_e, T_i, n_e and q) 1.5D simulations with a spatial grid of 50 points, have been realized with the JETTO transport code [25] using the GLF23 model (retuned version [21]) for heat and particle transport, with the objective of reproducing ITBs for a time interval sufficient for significant FFT expansion. Initial conditions have been chosen at t=5.6s, when well developed barriers were present on both T_e and T_i channels, while boundary conditions have been assumed constants referring to the experimental values at the top of the pedestal. Particular care has been used taking into account the non-negligible presence ~20% of ^{3}He (with respect to n_e) as impurity, relevant for the stabilisation mechanism through dilution. Clear ITBs have been reproduced for both ions and electrons, thanks to the ITG-TEM turbulence quenching by combined effects of $\omega_{E\times B}$ shearing rate, dilution, α-stabilisation and $s<0$. A predictive simulation of temperatures, density and current has been revealed crucial for triggering ITBs, because of the auto-consistency between the plasma profiles achieved by the model. Simulated values for electron and ion channels (Fig.2d), have given errors within ±13% with respect to measured temperatures; the radial position of the barriers is compatible with the experimental one, very close to q_{min}. The density profile n_e is predicted maintaining its average below an error of ±10%, but simulations have systematically shown central values and gradients higher than the experimental ones. The RF power deposition profiles for MC and FWLD are estimated according to previous transport simulations realized in order to match the experimental levels of the modulation analysis, using also the break-in slope method and the analysis of high frequency components [5,26]. The results of FFT analysis performed on simulated T_e time traces are reported in presence (Fig.2e) and without the transport barrier (Fig.2f). The latter one has been realized turning off the E×B shear and α stabilisation effects.

For the first time, perturbative analysis based on the first principles transport model GLF23 shows notable agreement not only with experimental evidences, but also with the simulations realized using a semi-empirical critical gradient length model. Contrary to the simulation without ITB, modulation amplitude and phase profiles recognize sharp discontinuities in presence of a transport

barrier, which definitely affects the propagation of heat perturbations. As observed in the experiments, the ITB behaves as a plasma region with very low χ_e and χ_e^{hp}, justifying the strong damping of both heat waves, while the discontinuity and the rise of the phase denote the slowing down of the heat pulses. The local decrease of χ_e^{hp} inside ITB reproduced by theory based gyro-fluid simulations with GLF23 is consistent with the critical gradient length hypothesis, according to the plasma is sub-critical with respect to an enhanced turbulence threshold with a consequent loss of stiffness. In the case instead corresponding to a plasma region of the ITB close to marginality and very stiff, i.e. with large χ_e^{hp}, the heat waves would travel without any damping by the barrier and with small phase changes. The reduction of transport levels originating from temperature and pressure gradients, but most of all the low values of the incremental heat diffusivity predicted by GLF23, are coherent with the hypothesis of the role of the turbulence threshold for a sub-critical transport inside the ITB region. In summary, first principles GLF23 simulations of perturbative electron heat transport deeply strengthen the main physical assumptions of critical temperature gradient length dynamics of transport processes.

4. EVIDENCE OF CONVECTIVE-LIKE BEHAVIOUR IN HEAT WAVE PROPAGATION IN JET ITB PLASMAS

Heat transport in JET plasmas in presence of significant ion and electron central heating, i.e. with large heat fluxes, is expected to be dominated by diffusive processes; this is indeed confirmed by power modulation results, which can be adequately reproduced according to a diffusive paradigm, both in L- and H-modes and also for the JET ITB plasmas previously described. This does not imply that small heat convection cannot be present, as predicted by the theory of electrostatic ITG-TEM turbulence [27, 28], but these cannot outside uncertainties be singled out of the dominant diffusive component of the heat flux. Specific studies in extreme experimental conditions of strong off-axis power and negligible core heat flux have given some evidence of the existence of heat convection (RTP [29], DIII-D [30], AUG [31] and FTU [32]). However it has also become clear [31] that signatures of convective terms can appear in heat wave propagation not only due to the existence of real heat convection but due to the dependence of the heat flux on temperature [33]. Such apparent convection terms can in some conditions become large and dominate the profiles of the heat wave amplitude (we remind that convection does not affect phases to first order), whilst the effect of real convection is generally small for the values expected from turbulence theory. One of these conditions, as pointed out in Ref. 20, takes place near the threshold in a critical gradient length model, when the value of the threshold is sufficiently high. In fact in such CGM model the heat diffusivity is expressed as

$$\chi_e = \chi_0 + \chi_s \frac{T_e}{eB}\frac{\rho_s}{R} q^{3/2}\left(\frac{R}{L_{Te}} - \kappa_c\right) H\left(\frac{R}{L_{Te}} - \kappa_c\right) \quad (1)$$

where H is Heaviside function, χ_0 represents the level of residual transport, $\rho_s = \sqrt{m_i T_e}/eB$, q is the

safety factor, χ_s is a dimensionless number giving the strength (stiffness) of the turbulent transport term assuming a gyro-Bohm normalisation and κ_c is the threshold. The dependence on temperature here appears explicitly in the $\chi_s q^{3/2}(T_e/eB)(\rho_s/R) = \lambda T_e^{3/2}$ term, in the L_{Te} term and possibly implicitly in the κ_c term. The apparent convective term is given by

$$U_e^{hp} = -\frac{\delta\chi_e}{\delta T_e}\nabla T_e^{pb} = -\frac{\lambda}{2}\,T_e^{3/2}\,\frac{\nabla T_e}{T_e}\left(\frac{R}{L_{Te}} - 3\kappa_c\right)H\left(\frac{R}{L_{Te}} - \kappa_c\right) \qquad (2)$$

where $U^{hp} < 0$ corresponds to an inward velocity. For a plasma just above the threshold $R/L_{Te} = \kappa_c$, Eq. (2) yields

$$U_e^{hp} = \approx -\frac{\lambda}{2}\,T_e^{3/2}\kappa_c^2 \qquad (3)$$

The latter relation shows how an intrinsic consequence of critical gradient length dynamics of heat transport is the existence, close to the turbulence threshold, of an apparent convective term. This is inward directed because of the inverse gradient length formulation (1), and proportional in magnitude to the square of the threshold value. In case of a plasma region slightly above κ_c, heat pulse propagation will become affected by an apparent heat pinch. As already predicted in Ref. 20, CGM formulation provides a visible effect of the apparent heat pinch close to the threshold when the value of κ_c is sufficiently high, due to its square dependence.

Direct evidence of the effect of such convective-like term was observed in AUG [31] in a region just inside the ECH off-axis deposition, i.e. close to the threshold. In this section we present cases also at JET where striking effects of this kind are observed when performing T_e modulation in ITB plasmas. The convective-like feature is observed just outside the ITB foot, indeed in a region near to the transition to ITB, i.e. close to threshold.

Figure 3 shows one example of discharge where modulation in an ITB plasma presents convective-like features. It is similar to the discharge in Fig.2 but with differences in toroidal field and ICRH deposition ($B_T = 3.6$ T, $I_p = 2.7$MA, $n_{e0} \sim 3\times10^{19}$ m^{-3}, ^{3}He ~ 21%, ICRH fr = 37MHz). In presence of the ITB (Fig.3b), Fourier expansion of T_e signals reveals a strong inflation of the amplitude modulation instead of decaying, in the region just outside the barrier. With respect to the power deposition location indicated by unperturbed minimum of φ, A values exhibit a maximum shifted inward very close to the ITB foot, while they are then efficaciously damped inside the ITB layer. From Fig.3c one can see that the effect completely vanishes when the barrier is lost, showing no distortions in the FFT profiles. Therefore, the effect is strictly linked to the presence of the ITB, although it takes place outside it. It is worth noting that the FFT expansion reported in Fig.3 has been performed carefully avoiding MHD activity inside the time interval of interest. Also spurious effects linked to possible collisional coupling with electrons, coming from the minority heating modulated component, have been taken into account; in this case ^{3}He resonance is located at $\rho = 0.08$ and can not influence the experimental modulation profiles. A last effect that could distort the amplitude and phase profiles is a modulated plasma

displacement in the laboratory reference frame, which in the presence of a significant temperature gradient would generate a spurious oscillation in the ECE measurements at a given radial position, as discussed in Ref. 6 for analogous ITB plasmas. Such signal would combine by vectorial addiction with the real T_e modulation, distorting its spatial profile. The presence of this effect can however be easily checked when measurements on both sides of the magnetic axis are available, as it is the case for these JET experiments, because the plasma displacement, being in antiphase on the two sides, introduces a visible asymmetry in the A and φ profiles on the two sides of the magnetic axis. The symmetry of the ECE measurements has been checked for shots exhibiting convective-like features and a good symmetry between the two field sides has been verified, allowing the conclusion that the shift observed between A maximum and φ minimum is a real transport effect.

1.5D transport simulations using the ASTRA code [34], have been performed in order to evaluate the convective term required for reproducing the experimental distortions of FFT expansions. These have revealed that if the effect were to be ascribed to real heat convection, a localized heat convective velocity with values up to more than $U \sim 15$ ms^{-1} would be necessary, whose level is theoretically justifiable in a very difficult way and moreover yields profiles of steady-state T_e and modulation that are inconsistent with each other.

Instead, simulations using no real heat pinch but the critical gradient model for the electron heat diffusivity, allowed us to reproduce well both the steady-state T_e profiles and the modulation results, including the very peculiar convective like feature in the amplitude profile. The simulations, focalised on electron heat transport, have considered as constants the experimental T_i and n_e profiles, while solving the equations for T_e and q (solving the current diffusion equation with the bootstrap term). For this one and the following simulations, the residual transport level χ_0 of formula (1) has been assumed $\chi_0 \approx 0.2$ m^2/s, while χ_s is typically $\chi_s \approx 0.5$. The key parameter in this kind of simulations is the assumed threshold κ_c for turbulence onset. Defining the profile of such critical value requires twofold considerations. The core region of the plasma, characterized by the presence of ITB, is dominated by suppression of turbulence, leading to increase of the threshold and consequent sub-critical transport. Consequently the turbulence threshold has been assumed arbitrarily higher inside the barrier region than in the rest of the plasma. The heat diffusivity in the region outside ITB foot will be instead turbulence dependent and sensitive to threshold values, whose profiles can be estimated according to theoretical predictions.

Several expressions for electrostatic instabilities thresholds have been derived; here we refer to the analytical formula derived for plasmas with dominant electron heating from linear gyrokinetic simulations for the Trapped Electron Modes (TEM) threshold [35]. This has been used in our simulations although strictly speaking in these JET ITB plasmas the condition $T_e > T_i$ is not satisfied (in the region of interest just outside the ITB $T_e \sim T_i$), and different instabilities TEM, ITG and ETG may be all active giving a complex situation. Still, it is expected that relevant component of turbulent electron heat flux should be ascribed to TEM instabilities, while ETG and ITG electron driven flux should be less relevant [12]. It must be here pointed out that purpose of these simulations is not to

obtain quantitative estimates of the turbulent electron heat flux, but to evaluate the consequence of critical gradient dynamics on heat wave propagation. The formula for TEM instability threshold derived in Ref.35 gives

$$\frac{R}{L_{Tcrit}} = \frac{0.357\sqrt{\varepsilon} + 0.271}{\sqrt{\varepsilon}} \left[4.90 - 1.31 \frac{R}{L_{Tcrit}} + 2.68s + \ln (1 + 20\, \nu_{eff}) \right] \qquad (4)$$

where ε=r/R is the local aspect ratio, R/L_n the normalized density gradient, s magnetic shear, while collisionality is characterized by $\nu_{eff} \approx 0.1R(Z_{eff}n_e)/T_e^2$. Starting from experimental data, the TEM threshold profile has been evaluated from relation (4); as explained in Ref. 35, this formula is obtained from a linear extrapolation to zero flux and the actual threshold is lower by about 70%, depending on R/L_n, therefore in the ASTRA simulations a correction factor of 0.7 has been applied to Eq.(4). This theoretically based profile has been assumed for the whole region outside the ITB foot, while inside the barrier the arbitrary high value κ_c=8 has been adopted. This distinction is also justified by the application limits of expression (4), which is not valid for explaining $s < 0$ conditions verified in the core region where the ITB is present.

Results of this kind of simulations for JET62085 using CGM are presented in Fig.4 and show good agreement with experimental evidences. The apparent convective term originating from critical gradient length dynamics can correctly reproduce the odd deviations from diffusive behaviour observed in the FFT profiles, even if no real convection is included in the model. As expected the effect refers locally to the region just outside the ITB foot, where $R\nabla T_e/T_e$ is close to turbulence threshold (see Fig.4), originating clear inflation of modulation amplitude away from power deposition location, visible from minimum of phase profile. The presence of appropriate level of U_e^{hp} for reproducing experimental inward heat wave growing is mainly due to two factors. The first and most important one is the high value of turbulence threshold foreseen by theoretical TEM predictions (4) just outside the barrier and acting through its square dependence in U_e^{hp}. The second one is linked to T_e dependence intrinsic in the collisionality term ν_{eff} of TEM threshold expression (4). Since the strength of the inward apparent pinch U_e^{hp} is proportional to $\partial\chi_e/\partial T_e$, logarithmic $1/T_e^2$ dependence inside TEM threshold formulation introduces an additional factor with respect to relation (2), increasing the inward apparent convection. It's worth noting that in ITB plasmas it is physically reasonable to assume the presence of a kind of connection, and not a sharp discontinuity, between two very different levels of turbulence threshold, the higher one corresponding to ITB stabilized region, and the lower ordinary one corresponding to turbulent plasma outside the barrier. Even this empirical consideration can lead to qualitatively reproduce the observed convective-like effects, thanks to local high threshold values just outside the ITB foot, if heat wave deposition is sufficiently close to this region. The good agreement between the simulation and the peculiar experimental data confirm that such convective-like effects represent a unique signature of critical temperature gradient nature of heat transport, particularly evident for its strong variance with respect to expected diffusive behaviour.

Simulations for the same discharge JET Pulse No: 62085 have been performed also using the

first principles transport model GLF23. The adopted approach for this kind of predictive simulations, is analogous to previous case of JET62077 (Fig.2) described in section III, where we refer for formulation details. With respect to experimental data, GLF23 simulations of JET62085 have systematically triggered ITBs characterised by a little radial outward shift ($\Delta\rho \sim 0.1$); this kind of effect simulating ITBs with the GLF23 was already observed, as pointed out in Ref.24. For this reason, in order to be closer to the experimental conditions where a modulated electron power source is located just outside the barrier, the MC profile has been arbitrarily translated of the same $\Delta\rho$. Obviously this requires particular care, but we remind that the MC heating remains a little perturbation with respect to the large amount of NBI power coupled to the electrons. Furthermore, the general purpose of these GLF23 simulations was not to achieve a quantitative agreement with experimental data, but to evaluate the existence of convective-like features inside a first principle gyro-fluid model and its accordance with the critical gradient length dynamics.

Plots of Fig. 5 refer to simulated profiles and FFT expansion of T_e signals; it is fundamental to remark that also in this case no real convective term has been imposed from outside. The comparison between the simulations with and without ITB is particularly relevant. In absence of transport barrier (Fig.5c), the modulation amplitude A shows its maximum slightly inward shifted with respect to the minimum of phase, where the power is effectively deposited. This is not a contradiction, but even it can represent the consequence of a plasma region that is above a moderately high turbulence threshold, thus yielding a small inward pinch according to critical gradient dynamics. Instead, when ITB is present (Fig.5b), the propagation of heat perturbations is more substantially affected by inward inflation. While the minimum of φ remains unperturbed, A continues increasing towards the barrier exhibiting its maximum very close to ITB foot. Even if the strength of heat wave growing is not as powerful as in CGM simulations, the effect refers locally to the region that connects the high turbulence threshold level of the barrier and the lower one of the rest of plasma. In summary, first principles GLF23 simulations predicts for some cases apparent convective features in heat wave propagation; as predicted by a transport regulated by critical gradient length dynamics, this effect is clearly enhanced by the presence of plasma locally above a high turbulence threshold, i.e. a situation likely verified in peculiar conditions just outside the ITB foot.

One obvious question is why these convective-like signatures exhibiting strong inflation of the heat wave amplitudes are observed in some JET ITB plasmas and not in others. JET62085 (Fig.3) has been chosen as representative case for its strong deviations from diffusive propagation of the heat perturbations, while JET62077 (Fig.2) is a representative case with no significant distortions. What is the different behaviour in apparently rather similar discharges due to ? The reasons of this evidence have been thoroughly investigated comparing theoretical profiles of TEM instability thresholds according to expression (4). The latter ones are plotted in Fig.6 for JET Pulse No's: 62077 and 62085, in their region of validity outside barriers, starting from experimental data referred to time when ITBs were fully developed. The discrepancies observed in turbulence threshold levels are consistent both with behaviour of perturbative heat transport predicted by critical gradient length

hypothesis and with the experimental results. In particular lower values of TEM thresholds for JET62077 with respect to JET62085 are foreseen, originating less significant apparent convection because of its square dependence from κ_c in expression (3). No inward heat wave inflation has in fact been experimentally observed in JET62077. On the other hand, the higher TEM instability threshold for JET62085 close to ITB can justify the peculiar heat wave propagation shown in Fig.3.

The discrepancies exhibited by the TEM threshold values are mainly due to the different position of the two ITBs, more inner for JET62085 than for JET62077 and acting through ε dependence, and to the destabilising effect of ∇n_e, more pronounced for JET62077. It must be stressed that the specific parametric dependence of the critical inverse gradient length model can determine as typical signatures both the presence and the level of convective-like features, in other ways not easily justifiable by theory, and particularly sensitive to the turbulence threshold value. Also first principles GLF23 simulations has been recognized as capable of reproducing convective-like distortions close to the barrier foot, exhibiting visible and enhanced heat wave inflation for JET62085 when the barrier is present, consistently with experimental results and with critical gradient length predictions based on different levels of TEM turbulence threshold.

5. OTHER PECULIAR EVIDENCES IN HEAT WAVE PROPAGATION IN JET ITB PLASMAS

Perturbative transport experiments in JET ITB plasmas have indeed revealed even more unexpected behaviour, as observed in JET62081, shown in Fig.7. For this discharge (B_T = 3.6T, I_p = 2.7MA, $n_{e0} \sim 3\times10^{19}$ m^{-3}, ^{3}He ~ 21%, ICRH fr = 37MHz) with off-axis MC deposition and analogous to the previous shots here described, the ITB is particularly weak and even unclear in the electron channel (Fig.7a). Analysis of heat wave propagation through FFT expansion has shown in this case a very peculiar double humped modulation amplitude profile (Fig.7b); only a first A maximum is consistent with phase minimum corresponding to power location, while the second one appears as odd effect at inner position close to the weak ITB foot. This unusual evidence is here reported for the first time, and its interpretation is not so immediate according to standard diffusive behaviour of transport. Two well separated maxima are visible in A profile, whilst the absence of two minima in the phase profile makes it at odds with diffusive behaviour. The inner peak can not be due to the presence of spurious minority heating component (^{3}He resonance at ρ=0.08), and the double humped profile systematically emerges when the weak ITB is present, and disappears without the ITB, as shown in Fig.7c, where a standard diffusive behaviour is recovered. The analysis is always performed avoiding MHD activity during considered time intervals. Very small inward shift of maximum of A during this last time interval can be reminiscent of faint apparent convection.

Transport simulations using ASTRA code, have demonstrated how these odd results can be understood and reproduced under critical temperature gradient length assumptions. As for JET62085, simulations of JET Pulse No: 62081 have been performed using CGM semi-empirical transport model predicting both T_e and q. Weak ITB in electron channel has been reproduced considering a turbulence

threshold profile whose values were only moderately increased inside the barrier region with respect to the rest of plasma (Fig. 8). FFT expansion of calculated temperature signals have shown that, apart from the ordinary A maximum linked to power deposition, a second more internal amplitude peak can be originated by the oscillation of T_e profile below and above turbulence threshold during the modulation cycle. Similar effect of cyclical oscillations around turbulence threshold driven by power modulation, has been considered in Ref.31 for investigation of electron heat pinches in AUG; the present results from a JET discharge are instead unique for the simultaneous presence of two amplitude peaks. The absence of huge temperature gradients in the experimental profiles of JET Pulse No: 62081, can suggest that plasma could be very close to turbulence threshold even inside the region characterized by the weak transport barrier. This situation can be regarded as intermediate between a well developed ITB with plasma fully below threshold, and a standard H-mode discharge where the plasma is instead fully above threshold. For these reasons the κ_c profile has been assumed in such a way that the power modulation cycle could induce a periodic transition inside the barrier region between turbulent and stabilized transport regime, driven by cyclical oscillation of the critical parameter $R\nabla T_e/\nabla T_e$ below and above threshold. Obviously the electron heat diffusivity level does not undergo dramatic discontinuities during the whole modulation cycle, and its time averaged value is indeed lower than in the rest of plasma, thus originating a modest steepening of temperature profile, i.e. the observed weak transport barrier.

The CGM formulation foresees that the heat wave travelling towards plasma core presents a first modulation amplitude peak in a region well above a moderately low threshold. In its propagation the heat pulse is then first locally quenched by the presence of an increased threshold level, but more internally it is re-amplified because of periodic access to turbulent regime; moreover being slightly above the higher threshold of this inner region during part of the modulation cycle can actually favour CGM-driven convective-like growing of the heat perturbation. Finally the heat pulse is definitely damped in the core region. In other words, the inner amplitude maximum is effectively a local heat pulse amplification occurring at the modulation frequency, due to backwards transition from a stabilized transport branch to a turbulent one having place during part of the modulation cycle. This effect is a characteristic feature of the critical temperature gradient length hypothesis, and necessarily requires the key concept of a threshold for onset of enhanced turbulent transport. Furthermore this feature is consistent with a 2^{nd} order transition scheme for ITB formation. The concept of phase transition can be applied to ITB formation using as order parameter the electron heat flux, whilst the plasma response is R/L_T. 1^{st} order means that R/L_T experiences a discontinuity at the transition while it stays continuous for a 2^{nd} order transition[5]. This argument will be also deepened in the following section. In this case the heat pulse growth has been observable for the peculiar conditions of a weak transport barrier, i.e. a region where the plasma can be cyclically destabilized by the incoming hot heat pulses above a moderately increased turbulence threshold. In spite of qualitative agreement with experimental data obtained by this CGM simulation, finer refinements are beyond the scope of this study. The attention has instead to be focused onto the capability by such a crude model for electron heat diffusivity

expressed by (1), of easily reproducing an experimental evidence which is not only peculiar, but also not ascribable to presently known diffusive transport mechanisms. On the contrary, the hypothesis of existence of critical temperature gradient length for turbulent transport onset, is capable of conciliating under the same basic assumptions both standard diffusive behaviour and odd distortions in heat wave propagation emerged for these discharges. Within this framework a crucial role is assumed by the turbulence threshold profile. In particular, both the convective-like heat pulse inflation of JET Pulse No: 62085 and the second internal amplitude peak exhibited by JET Pulse No: 62081 appear as distinctive signature of critical gradient length nature of heat transport.

6. ASYMMETRIES BETWEEN HOT AND COLD HEAT PULSE PROPAGATION ACROSS ITB

Before performing power modulation experiments, initial perturbative transport studies for probing JET ITBs were done using Cold Pulses (CP), induced by Ni laser ablation or shallow pellet injection and travelling from the edge towards plasma core [14]. These experiments have shown how the cold pulse undergoes a clear amplification when crossing the ITB foot, i.e. in a region evidently characterized by the presence of the barrier, while exhibiting a strong damping further inside. In particular this kind of results has been identified as one of the clearest proofs in favour of a 2^{nd} order transition scheme for ITB formation [5]. The CP growth in the outer ITB region can in fact be explained by a local χ_e increase originated by a backwards switch from below to above turbulence threshold, because of the enhanced ∇T_e carried by the arrival of the cold pulse. On the contrary, a 1^{st} order scheme, characterized by bifurcation and hysteresis in the back-transition, would not reproduce at all the same effect.

The evidence presented in section IV, in analogous JET ITB plasmas, could cast the doubt that also the cold pulse amplification could be due to convective-like effects rather than to back-transition. It must be here stressed that the experimental CP amplification is clearly observed inside the ITB region, where the plasma was formerly well below threshold (see Fig.8-10 of Ref. 14), while the convective-like effect takes place only in presence of a region slightly but always above threshold, i.e. outside the barrier foot. Nevertheless, in order to gain a correct and more complete understanding, it's still very useful to verify in which measure these two effects can be discriminated according to CGM. In fact, from the point of view of the transport model, the apparent convection term predicted by critical gradient length dynamics does not distinguish between cold and hot pulses, inducing the amplification of both kinds of heat waves in the region just region outside the ITB foot if the threshold is sufficiently high. This may originate possible ambiguities in the experimental identification of the cold pulse amplification due to back-transition, even if this is an effect taking place inside the ITB foot. This distinction is not academic because, if the CP growth was only due to CGM apparent convection, this would invalidate the conclusion expressed in Ref.5 that the evidence of cold pulse growth implies a local inverse transition within a 2^{nd} order scheme. These two different mechanisms, even within the same framework of critical gradient length model and originating similar effects, have to be correctly recognized in order to derive coherent conclusions from the experimental evidences.

Transport simulations using CGM model with ASTRA code have been performed, focusing the attention on the effects and differences in the propagation of both cold and hot single heat pulses from the plasma edge towards the ITB. With this purpose, exactly the same conditions of the CGM simulation for JET Pulse No: 62085 (Fig.4, see section IV for details) have been used, i.e. resulting in relevant apparent convection thanks to the assumed κ_c profile derived from TEM threshold predictions. Instead of the modulated power source, the propagation of a single cold (or hot) heat pulse has been simulated imposing time evolving T_e boundary conditions analogous (or reversed with respect to unperturbed temperature) to the experimental values of discharges with Ni injection considered in Ref.14. These simulations obviously refer to no real discharges, but they represent very useful fictitious experiments for integrating the previous results into a wider vision on critical gradient length signatures.

Results of Fig.9 show a clear asymmetry between the propagation of a cold pulse in an ITB with respect to a hot one (HP). As expected, the ΔT_e time evolution referred to a hot pulse is fully consistent with the previous power modulation simulation (Fig.4): travelling from the plasma periphery the heat pulse is inflated by the effect of apparent CGM U_e^{hp}, whose strength is enhanced with higher values of κ_c. The amplification effect plays only in the region above threshold reaching its maximum just outside the ITB foot, while the hot pulse is strongly damped where the plasma becomes sub-critical, i.e. inside the barrier. On the other side, the CP propagation points out a first amplification above threshold symmetrically with respect to the hot pulse, but when crossing the ITB it is able to destabilize the formerly sub-critical outer part of the barrier inside its foot, highlighting a second inner amplification of the CP. Only more inside, the barrier is unaffected by the arrival of the cold pulse which is here effectively damped. The CP growth inside the barrier foot is indeed due to back-transition, which is obviously an asymmetric effect with respect to the sign of the pulse, since only the increase in ∇T_e carried by a cold pulse can lead to destabilization.

The asymmetries presented by these simulations between hot and cold pulse propagation in ITB plasmas clarify the different and distinguishable nature of the heat wave amplification for both the experimental evidences of CP growth inside the ITB region, and of convective-like effects outside of it. These results fully confirm the hypothesis expressed in Ref.5, demonstrating how even in conditions of remarkable CGM-driven apparent convection, the cold pulse amplification inside the ITB foot is visible and directly due to an inverse transition to a turbulent transport branch within a 2^{nd} order scheme for ITB formation. At the same time this exercise gives an interesting insight about the differences/similarities in the propagation of cold and heat pulses in two distinct transport regimes, below and above threshold.

CONCLUSIONS

New results coming from electron heat wave propagation experiments in JET ITB plasmas showing several peculiar signatures of critical gradient length transport dynamics have been presented in this paper.

For the first time the experimentally observed strong damping of the heat waves meeting the

ITB has been reproduced with fully predictive simulations using theory based gyro-fluid GLF23 model (Fig.2). This result confirms that the internal transport barrier behaves like a plasma region characterized by a significant reduction of incremental heat diffusivity and loss of stiffness, according to the hypothesis of sub-critical transport with respect to a local increase of turbulence threshold. Peculiar observations have been reported in some JET ITB plasmas (and not present in the absence of the ITB) of a strong inflation of the heat wave just outside the ITB foot, with clear deviations from expected diffusive behaviour in favour of relevant convective-like features. Such features, which would require huge heat convective velocity not easily theoretically justifiable, are on the other hand fully accounted by a model based on the existence of a critical temperature gradient length for onset of turbulent transport. This leads to the presence of an apparent convection for heat pulse propagation in the proximity of a sufficiently high threshold. Good reproduction of the data was obtained using a semi-empirical Critical Gradient length Model (CGM) for the electron heat diffusivity χ_e and assuming a threshold profile based on linear gyro-kinetic predictions for TEM instability threshold. Simulations of discharges exhibiting convective-like features have been performed also using the first principle GLF23 transport model. Remarkably, the peculiar heat wave inflation located just outside the ITB foot was reproduced also by GLF23, together with the disappearance of this feature in the absence of ITB.

Even more peculiar experimental observations have revealed the presence of two separate amplitude peaks in the heat wave propagation, where only the first one is consistent with power deposition location. The appearance of the second and inner maximum can be reproduced as the effect of periodic transitions below and above the turbulent transport threshold, driven by oscillations of T_e profile across threshold in presence of a weak ITB. Re-crossing of turbulence threshold with consequent local χ_e increase can also be obtained by destabilizing the outer part of the barrier through the propagation of cold pulses, which then undergo an inflation effect, as observed in earlier experiments. CGM simulations have allowed the identification of convective-like amplification and cold pulse growth due to back-transition as separate and distinguishable mechanisms. Therefore, they have confirmed the former hypothesis that cold pulse growth inside the ITB foot is due to back-transition, which favours a 2^{nd} order transition scheme for ITB formation. In summary, a variety of new and peculiar evidences from heat wave propagation in JET ITB plasmas can be consistently interpreted as signatures of the existence of a critical gradient length for the onset of turbulent transport. These observations complement original observations in AUG and other tokamaks demonstrating the key importance of the threshold concept to reach a consistent understanding of perturbative transport results in L- and H-mode plasmas. The present JET results extend these evidences to plasma regimes with Internal Transport Barriers.

REFERENCES

[1]. J.W. Connor, T. Fukuda, X. Garbet *et al.*, Nucl. Fusion **44**, R1-R49 (2004)

[2]. C.D. Challis, Plasma Phys. Controlled Fusion **46**, B23-B40 (2004)

[3]. X. Litaudon, E. Barbato, A. BÈcoulet *et al.*, Plasma Phys. Controlled Fusion **46**, A19-A34 (2004)
[4]. T. Tala and X. Garbet, Comptes Rendus Physique **7**, 622-633 (2006)
[5]. P. Mantica, D. Van Eester, X. Garbet *et al.*, Phys. Rev. Lett. **96**, 95002 (2006)
[6]. A. Marinoni, P. Mantica, D. Van Eester *et al.*, Plasma Phys. Controlled Fusion **48**, 1469-1487 (2006)
[7]. P. Mantica and F. Ryter, Comptes Rendus Physique **7**, 634-649 (2006)
[8]. F, Ryter, C. Angioni, A. G. Peeters, F. Leuterer, H.-U. Fahrbach, W. Suttrop and ASDEX Upgrade Team *et al.*, Phys. Rev. Lett. **95**, 085001 (2005)
[9]. F. Ryter, G. Tardini, F. De Luca, *et al.*, Nucl. Fusion **43**, 1396-1404 (2003)
[10]. X. Garbet, P. Mantica, C. Angioni, *et al.*, Plasma Phys. Controlled Fusion **46**, B557-B574 (2004)
[11]. X. Garbet, P. Mantica, F. Ryter, *et al.*, Plasma Phys. Controlled Fusion **46**, 1351-1373 (2004)
[12]. F. Ryter, Y. Camenen, J. C. DeBoo, *et al.*, Plasma Phys. Controlled Fusion **48**, B453-B463 (2006)
[13]. G. T. Hoang, C. Bourdelle, X. Garbet *et al.*, Phys. Rev. Lett. **87**, 125001 (2001)
[14]. P. Mantica, G. Gorini, F. Imbeaux, *et al.*, Plasma Phys. Controlled Fusion **44**, 2185-2215 (2002)
[15]. M.J. Mantsinen, M. Mayoral, D. Van Eester *et al.*, Nucl. Fusion **44**, 33-46 (2004)
[16]. P. Mantica, X. Garbet, F. Imbeaux *et al., Proceedings of the 30th EPS Conference, St. Petersburg 2003*, in Europhysics Conference Abstracts, European Physical Society, Vol. **27A** O-3.1A (2003)
[17]. P. Mantica, X. Garbet, C. Angioni *et al., Proceedings of the 20th International Conference on Fusion Energy, Villamoura 2004*, International Atomic Energy Agency (IAEA), Vienna, EX/ P6-P18 (2004)
[18]. A. Manini, F. Ryter, C. Angioni, *et al.*, Plasma Phys. Controlled Fusion **46**, 1723-1743 (2004)
[19]. P. Mantica, F. Imbeaux, M. Mantsinen *et al., Proceedings of the 31st EPS Conference, London 2004*, in Europhysics Conference Abstracts, European Physical Society, Vol. **28G** p. 1.154 (2004)
[20]. F. Imbeaux, F. Ryter and X. Garbet, Plasma Phys. Controlled Fusion **43**, 1503-1524 (2001)
[21]. J.E. Kinsey, G.M. Staebler and R.E. Waltz, Phys. Plasmas **12**, 052503 (2005)
[22]. R.E. Waltz, G.M. Staebler, W. Dorland, G. W. Hammett, M. Kotschenreuther and J. A. Konings, Phys. Plasmas **4**, 2482 (1997)
[23]. R.E. Waltz and R. Miller, Phys. Plasmas **6**, 4265 (1999)
[24]. T. Tala, F. Imbeaux, V.V. Parail**,** *et al.*, Nucl. Fusion **46**, 548-561 (2006)
[25]. G. Genacchi and A. Taroni, 1988 JETTO: *A free boundary plasma transport code (basic version) Rapporto* ENEA RT/TIB 1988(5)
[26]. D. Van Eester, Plasma Phys. Controlled Fusion **46**, 1675-1697 (2004)

[27]. X. Garbet, N. Dubuit, E. Asp, Y. Sarazin, C. Bourdelle, P. Ghendrih, and G. T. Hoang, Phys. Plasmas **12**, 082511 (2005)
[28]. P. Mantica, A. Thyagaraja, J. Weiland, G. M. D. Hogeweij, and P. J. Knight., Phys. Rev. Lett. **95**, 185002 (2005)
[29]. P. Mantica, G. Gorini, G. M. Hogeweij, N. J. Lopes Cardozo, and A. M. Schilham, Phys. Rev. Lett. **85**, 4534 (2000)
[30]. T. C. Luce, C. C. Petty, and J. C. de Haas, Phys. Rev. Lett. **68**, 52 (1992)
[31]. P. Mantica, F. Ryter, C. Capuano, H. U. Fahrbach, F. Leuterer, W. Suttrop, J. Weiland and ASDEX-Upgrade Team, Plasma Phys. Controlled Fusion **48**, 385-406 (2006)
[32]. C. Sozzi, *Proceedings of the 18th International Conference on Fusion Energy, Sorrento 2000*, International Atomic Energy Agency (IAEA), EX/P5-13 (2000)
[33]. A. Jacchia, P. Mantica, F. De Luca and G. Gorini, Phys. Fluids B **3**, 3033 (1991)
[34]. G. Pereverzev and P. N. Yushmanov, IPP Report, 5/98 (2002)
[35]. A. G. Peeters, C. Angioni, M. Apostoliceanu, F. Jenko, F. Ryter and the ASDEX Upgrade team, Phys. Plasmas **12**, 022505 (2005)

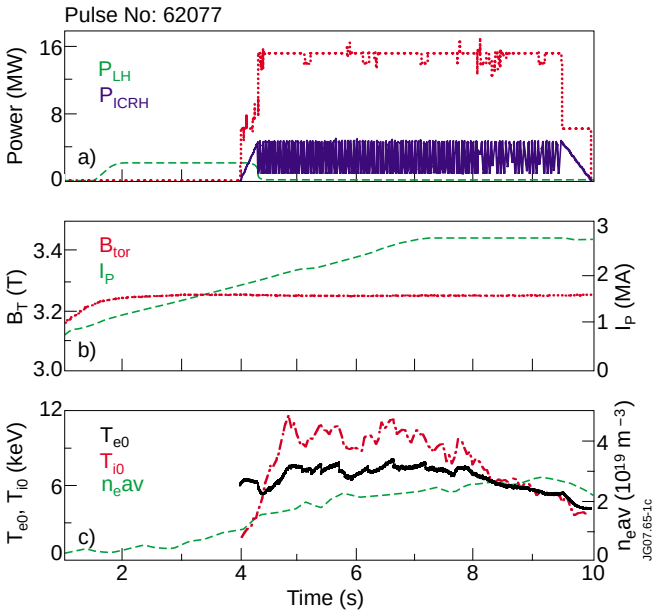

Figure 1: (a) Typical heating scheme for power modulation experiments with ITBs for JET Pulse No: 62077. (b) Time evolution of B_T and plasma current I_p for the same discharge. (c) Time traces of T_{e0}, T_{i0} and volume averaged n_e for JET Pulse No: 62077.

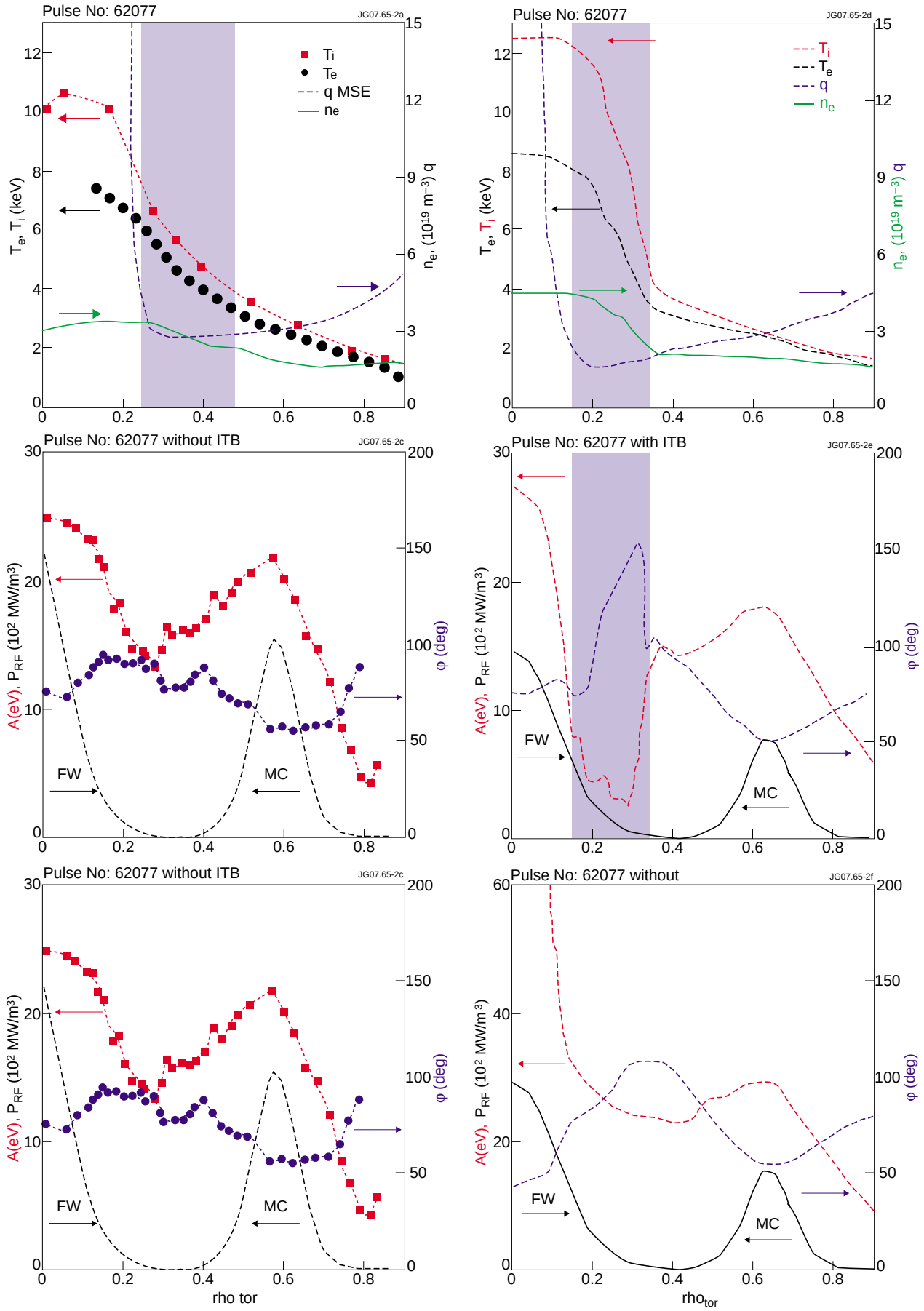

Figure 2: (a) Experimental profiles of T_e, T_i, n_e and q for JET Pulse No: 62077 (3.25 T/2.6 MA, ^{3}He ~ 20%, ICRH fr = 37MHz), with ITB region highlighted. (b) Profiles of Fourier component performed on T_e time traces of A [squares (red online)] and j [circles (blue online)] at the modulation frequency (20Hz) during the time interval 5.5-5.7s. Estimated RF power deposition profiles are also plotted (dashed black line). (c) Analogous FFT results without ITB. (d) Profiles of T_e, T_i, n_e and q simulated using gyro-fluid GLF23 model. (e) Profiles of Fourier expansion performed on T_e time traces simulated with GLF23. (f) Analogous FFT results using GLF23 without ITB.

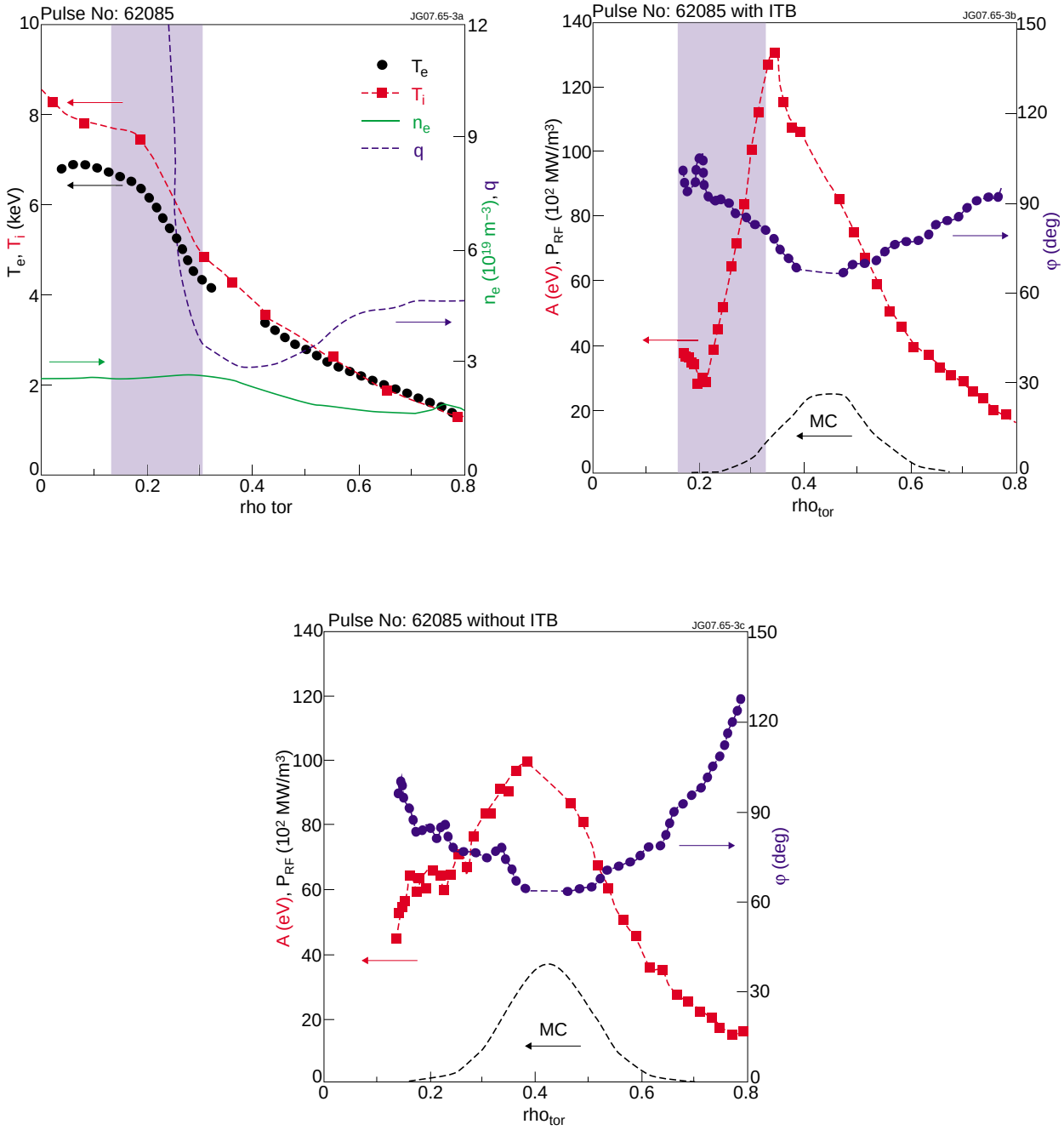

Figure 3: (a) Experimental profiles of T_e, T_i, n_e and q for JET Pulse No: 62085 (3.6 T/2.7MA, ^{3}He ~ 21%, ICRH fr = 37MHz), with ITB region highlighted. (b) Profiles of Fourier component of A [squares (red online)] and φ [circles (blue online)] at the modulation frequency (20 Hz) during the time interval 4.83-5.03s. Estimated RF power deposition profile is also plotted (dashed black line). (c) Analogous FFT results for the same shot for the time interval 6.8-7s without ITB.

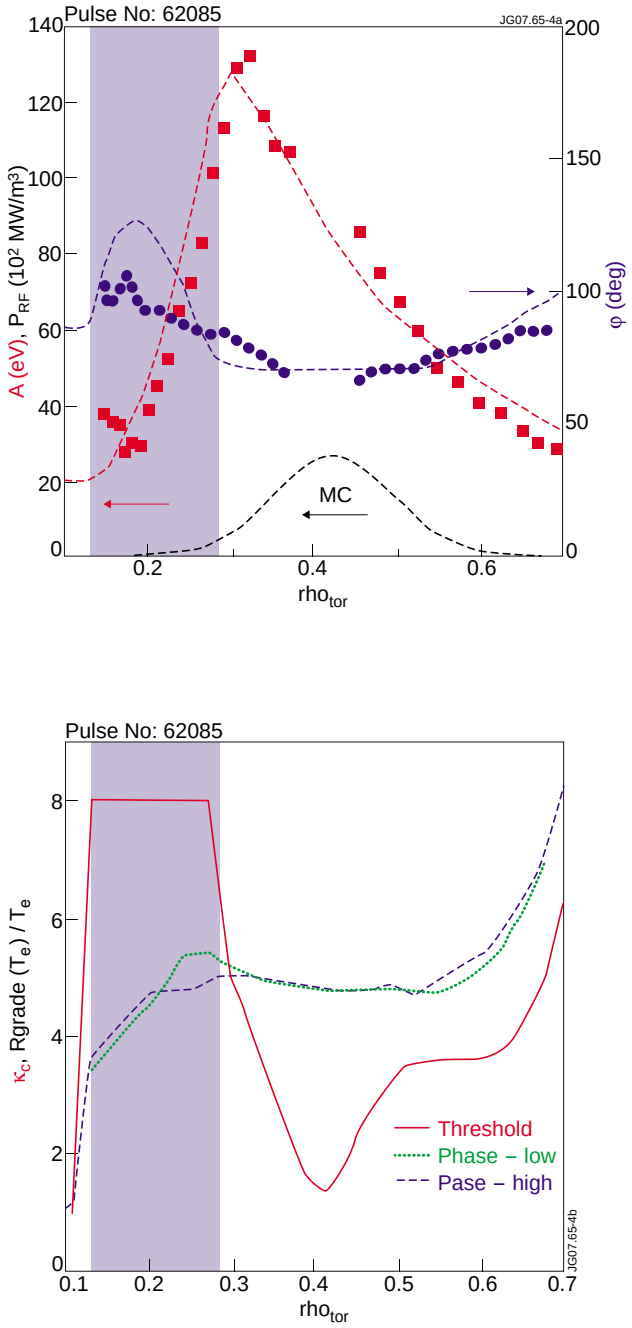

Figure 4: Simulation of JET Pulse No: 62085 using CGM transport model. (a) Experimental (dots) and simulated (lines) FFT profiles of A (red online) and φ (blue online); power deposition profile is also plotted (dashed black line). (b) Profile of turbulence threshold κ_c (red online) used for CGM simulation, calculated according to TEM theoretical instability threshold (4) (multiplied by 0.7) in the region outside ITB, and assumed κ_c=8 inside ITB; profiles of simulated $R\nabla T_e/T_e$ (dashed lines) are also plotted for both high and low power phase of the modulation cycle.

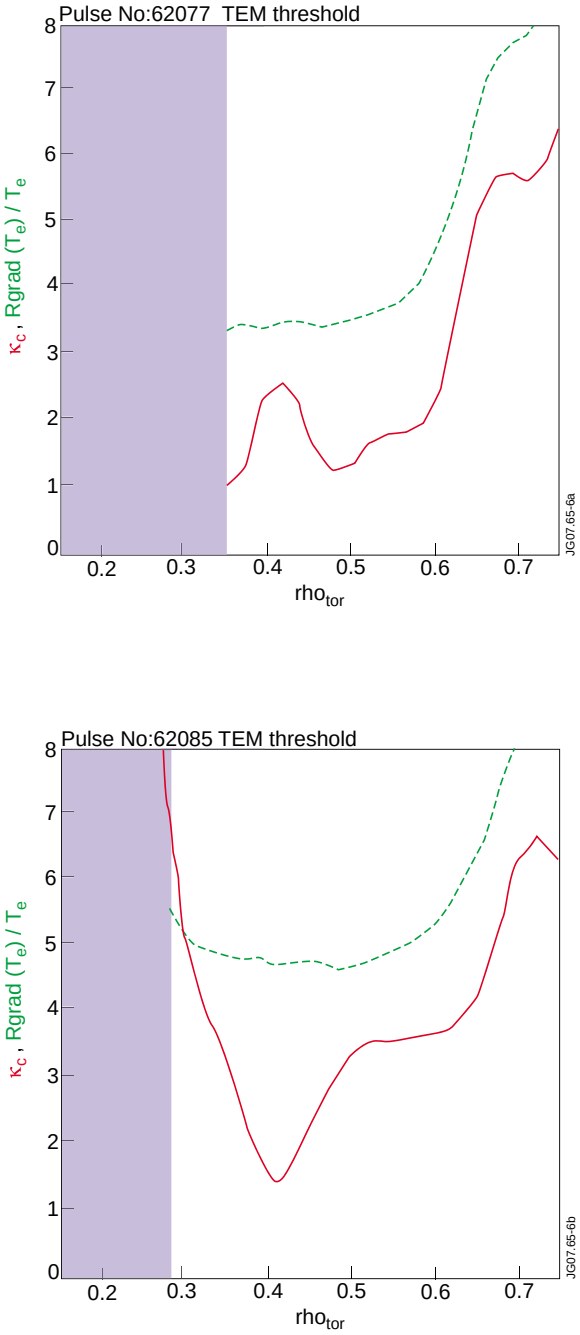

Figure 6: Profiles of Trapped Electron Modes (TEM) instability threshold κ_c (continuous lines) according to formulation (4) derived from linear gyrokinetic simulations (Ref.34) and profiles of simulated R/L_{Te} (dashed lines) for shots JET Pulse No: 62077 (a) and JET Pulse No: 62085 (b). Highlighted areas correspond to ITB regions, where threshold profiles according to (4) are not valid.

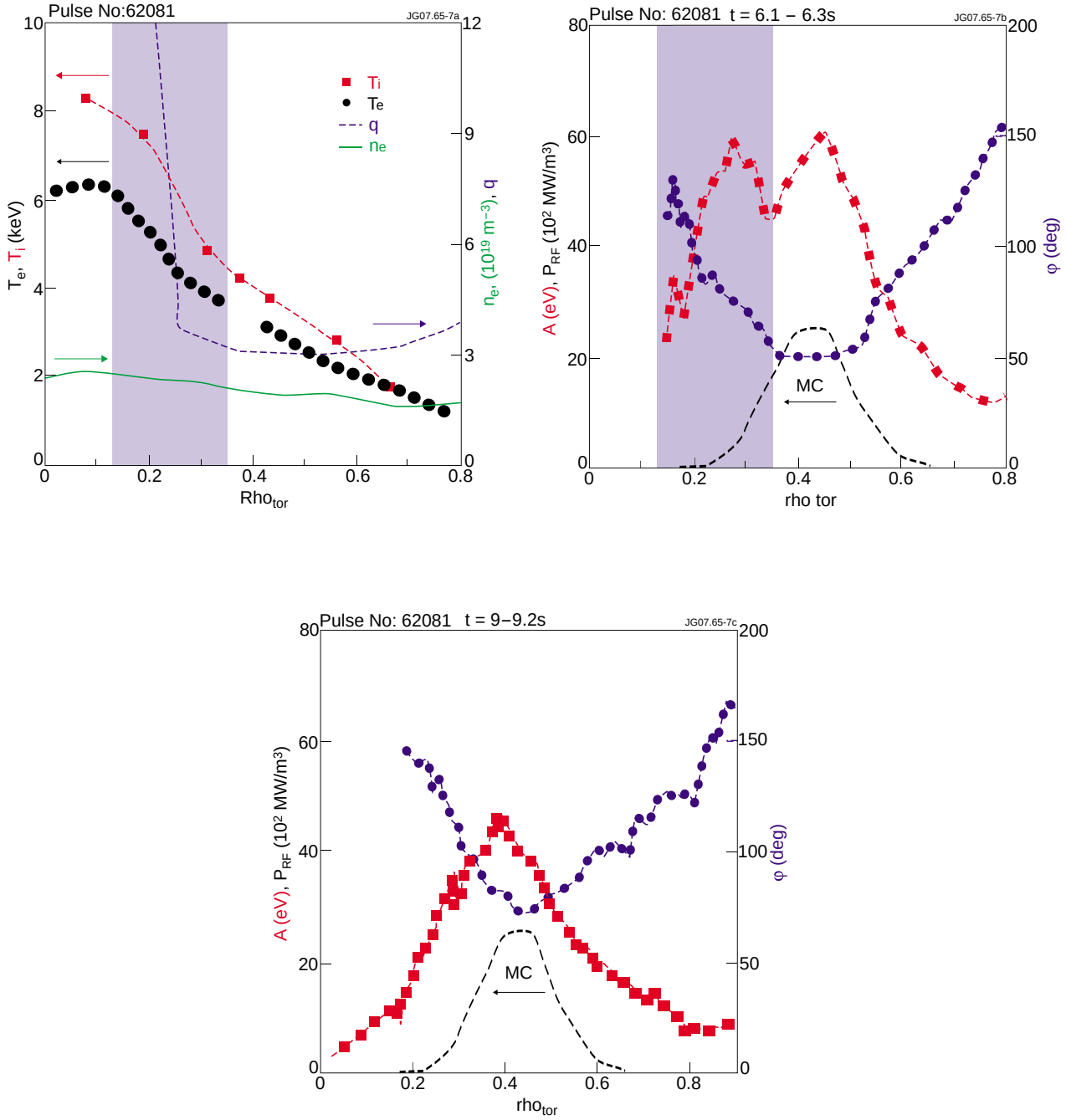

Figure 7: (a) Experimental profiles of T_e, T_i, n_e and q for JET Pulse No: 62081 (3.6 T/2.7MA, ^{3}He ~ 21%, ICRH fr = 37MHz), with weak internal ITB. (b) Profiles of Fourier component of A [squares (red online)] and φ [circles (blue online)] at the modulation frequency (20Hz) during the time interval 6.1-6.3s. Estimated RF power deposition profile is also plotted (dashed black line). (c) Analogous FFT results for the same shot in a later phase when the weak barrier is definitely lost.

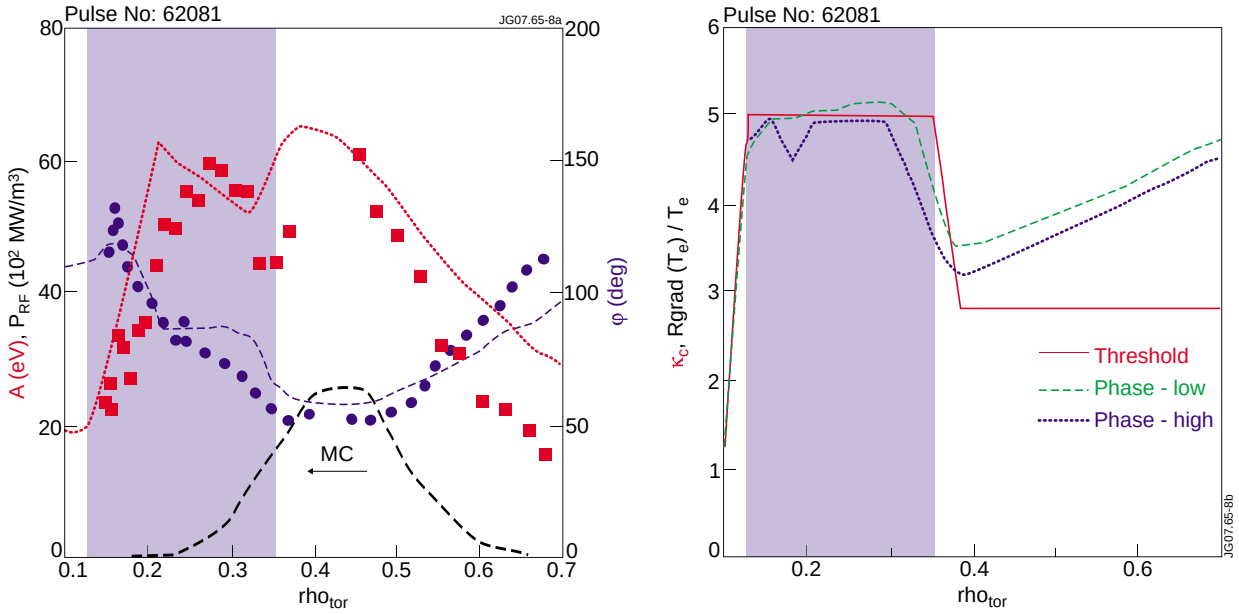

Figure 8: Simulation of JET Pulse No: 62081 using CGM transport model: (a) Experimental (dots) and simulated (lines) FFT profiles of A (red online) and φ (blue online). (b) Particular of turbulence threshold κ_c profile (red online) assumed for simulation, locally moderately increased in order to reproduce a weak barrier; the simulated $R\nabla T_e/T_e$ (dashed lines) periodically oscillates above and below κ_c between the high and low phase of the modulation cycle.

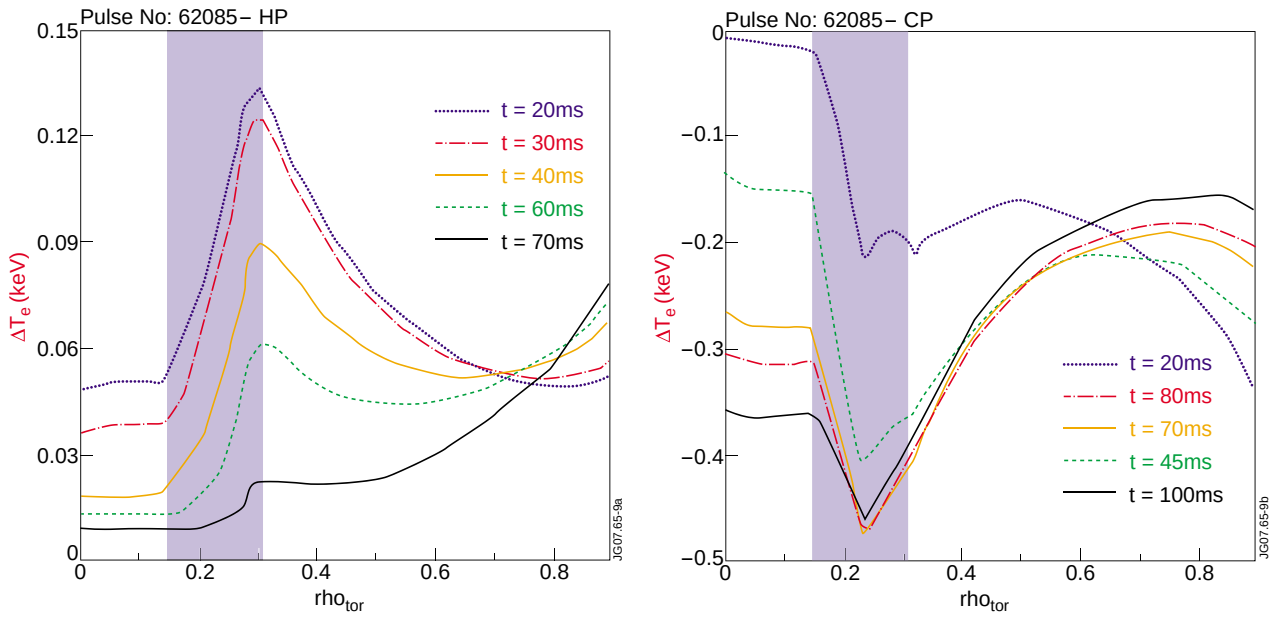

Figure 9: Simulation of heat pulses propagation travelling from plasma edge towards the ITB (region highlighted) in JET Pulse No: 62085 using CGM transport model. (a) ΔT_e (referred to steady state temperature) at several time instants after the Hot Pulse (HP) start. (b) Analogous ΔT_e time evolution for the propagation of a Cold Pulse (CP).